A COMPARATIVE STUDY OF THE STRUCTURAL AND OPTICAL PROPERTIES OF NIO NANOPARTICLES DOPED WITH CERIUM AND SAMARIUM

Swati R. Gawali
Department of Physics, CES's Dr. Arvind B. Telang Sr. College, Nigdi, Pune.

Abstract: *In the present work, nickel oxide nanoparticles, Ce doped nickel oxide nanoparticles and Sm doped nickel oxide nanoparticles are synthesized using the simple sol gel technique. The influence of doping of Ce and Sm (1.00 atomic %) on the crystalline structure and optical properties of NiO nanoparticles was investigated. The samples were characterized for structure, phase and morphology by XRD, EDAX and SEM techniques. The XRD patterns confirmed the formation of face centered cubic structure for undoped NiO nanoparticles, Ce doped NiO (CNO) nanoparticles and Sm doped NiO (SNO) nanoparticles. The average crystalline size of the as prepared samples were calculated and reported as were 27 nm for undoped NiO nanoparticles, 35 nm for CNO nanoparticles and 33 nm for SNO nanoparticles. The Hall-Williamson analysis is used to estimate the average crystalline size and lattice strain induced due to the substitution of cerium and samarium in the prepared sample. The SEM images reveal spherical morphology with the formation of mono-sized particles. The optical properties were compared by measuring the band-gap energy with UV–visible spectroscopy technique. The band gap of CNO nanoparticles (3.5 eV) was found to be lower than that of the undoped NiO nanoparticles (3.61 eV) whereas for SNO nanoparticles (3.77 eV) it was found to be more than that of the undoped NiO nanoparticles (3.61 eV).*

***Keywords*: Doping, CNO Nanoparticles, SNO Nanoparticles, Sol-Gel method, Optical Properties**

1. Introduction:

Recently, transition metal oxide nanostructures have attracted researchers due to their wide applications in the field of biomedicine, spintronics, telecommunication and energy. The development of these materials is mainly based on their use in the sustainable development for benefit of the mankind. Nickel oxide is a p-type semiconductor with wide band gap energy of 3.6 to 4.0 eV [1]. This material is explored in many applications such as catalysts [2], rechargeable batteries [3], p-type transport conducting films [4], electro chromic coatings [5], giant magneto-resistance (GMR) material [6], fuel cells [7], gas sensors [8] and solar cells [9]. The nanoparticles of NiO can be synthesized by various methods such as chemical vapor deposition, sol-gel, sputtering, micro emulsion precipitation method and so on. The properties of this material can be tailored with different approaches like addition of noble metals [10-13], doping of metal oxide catalyst [14,15], developing hybrid materials [16] and the design of nanostructures with large surface area, different morphologies and nanoscale sizes [17,18]. Among these approaches the simplest and extensively used method to modify the properties of the parent material is doping of noble metals. It is observed that the dopants segregate on the nanostructured metal surface or they can be incorporated into the lattice, where the dopants can be substitutional or interstitial or both. In general, doping of a rare earth metals like La, Ce, Sm and Yb are used to modify the electronic structure of transition metal oxide nanoparticles [19, 20, 21].

NiO has a poor electrical conductivity. Hence it cannot be used in the applications of super capacitor. But cerium has good capacitive characteristic due to the higher redox ability between Ce^{3+} and Ce^{4+} based on oxidizing and reducing conditions and it could easily form oxygen vacancies with relatively high mobility of bulk oxygen species [16, 22]. Therefore, doping Ce into NiO nanoparticles can enhance the electrical conductivity of NiO many times. The free oxygen species generated during the redox reaction between Ce^{3+} and Ce^{4+} can also be used in altering the gas sensing properties of the pure NiO nanoparticles. The trivalent Samarium (Sm^{3+}) ion is under extensive research due to its applications in high-density optical storage, color displays in different fluorescent devices, undersea communication and bright emission in red-orange regions leads to visible solid-state lasers [23]. Earlier, several authors reported physical, photoluminescence studies on Sm^{3+} doped with different host materials. Samarium exhibits a promising characteristic for spectral hole burning studies [24].

In the present work we have doped Ce and Sm into NiO nanoparticles and studied the effect of doping on the structure of NiO nanoparticles. The material is also tested for optical properties in comparison with the undoped NiO nanoparticles. Particle size and phase were determined by using XRD and EDAX. The optical measurements were also taken to study the effect of doping on band gap energy. All these results are discussed in this paper in detail.

2. Experimental Details:

Undoped nickel oxide nanoparticles, cerium doped nickel oxide nanoparticles and samarium doped nickel oxide nanoparticles were synthesized by the simple sol-gel method. The chemicals used as precursors were nickel nitrate hexahydrate ($N_2NiO_6{\cdot}6H_2O$), cerium nitrate hexahydrate ($Ce(NO_3)_3{\cdot}6H_2O$), samarium nitrate hexahydrate ($Sm(NO_3)_3{\cdot}6H_2O$) and oxalic acid ($C_2H_2O_4{\cdot}2H_2O$). Ethanol was used as the solvent. All the chemicals used were of analytical grade obtained from Merck Company Ltd. and used as received.

Preparation of undoped NiO nanoparticles:

Under continuous stirring and heating a solution of nickel nitrate was prepared in ethanol for preparing undoped NiO nanoparticles. A homogeneous solution of oxalic acid was also prepared in ethanol and was added to the nickel nitrate solution drop by drop. Heating and stirring were continued

for about 15 min. Thereafter, stirring was stopped, but heating was continued until the formation of a gel. The green-colored gel was dried overnight in air. The as-prepared sample was annealed at 400 °C for two hours.

Preparation of Ce doped NiO nanoparticles:

To prepare the samples of Ce doped NiO, 0.4 M solution of cerium nitrate was prepared in ethanol. Under continuous stirring this solution was slowly added into the nickel nitrate solution and then the solution of 0.08 M oxalic acid solution was added in this solution. The process of heating and stirring was continued for about 15 min. Thereafter, stirring was stopped, but heating was continued until the formation of a gel. The gel was dried overnight in air. The as-prepared sample was annealed at 400 °C for two hours. In particular the molar percentage of cerium with respect to nickel were taken to be 1% and thus Ce doped NiO nanoparticles were prepared.

Preparation of Sm doped NiO nanoparticles:

To prepare the sample of Sm doped NiO, solution of samarium nitrate was prepared in ethanol. Under continuous stirring this solution was slowly added into the nickel nitrate solution and then oxalic acid solution was added in this solution. The process of heating and stirring was continued for about 15 min. Thereafter, stirring was stopped, but heating was continued until the formation of a gel. The gel was dried overnight in air. The as-prepared sample was annealed at 400 °C for two hours. In particular the molar percentages of samarium with respect to nickel was taken to be 1% and thus Sm doped NiO nanoparticles were prepared.

Characterization:

The phase, structure and average grain size of the as-prepared samples were characterized by X-ray diffraction at Central Facility, Garware College, Pune. EDAX characterization of the undoped NiO, Ce doped NiO nanoparticles and Sm doped NiO nanoparticles were conducted at the Physics Department, SPPU, Pune. The band-gap energies of all the samples were determined from the UV–vis-spectroscopy measurements carried out at the Central Facility at Garware College, Pune.

The crystal structure and phase of pure NiO, CNO and SNO nanoparticles were investigated by X-ray powder diffraction (with CuK_α radiation; λ = 1.5406 Å.) The lattice parameters a, b and c of samples were calculated by using the following equations [25, 26].

$$2d_{hkl}Sik\theta = k\lambda$$

$$\frac{1}{d_{hkl}^2} = \frac{4}{3}\left[\frac{h^2 + hk + k^2}{a^2}\right] + \frac{l^2}{c^2}$$

where λ = The wavelength of the XRD,
n = The order of diffraction (for first order n = 1),
d_{hkl} = The interplanar spacing
hkl = The Miller indices.

The average crystallite size (D) of the prepared samples was determined from the XRD data using the Scherrer's equation [25]

$$D_{hkl} = \frac{0.94\lambda}{\beta_{hkl}\,Cos\theta}$$

where $\lambda_{CuK\alpha}$ = 1.5406 Å,
β_{hkl} = full-width at half maximum intensity (FWHM) of the XRD peaks in radians
θ = the Bragg's angle of the diffraction peak.

The optical properties of the prepared samples were investigated using UV–visible spectrophotometer in the wavelength range of 200 – 500 nm. The direct transitions band gap energies (Eg) were calculated by using the Tauc's equation [26, 27]

$$\alpha = \frac{\beta(hu - E_g)^{\frac{1}{2}}}{hu}$$

where α = the optical absorption coefficient,
β = a constant,
h = the Planck's constant
ν = the wave frequency.

3. Results and Discussions:

In this section we will discuss the XRD, EDAX and optical properties of the undoped NiO nanoparticles, CNO nanoparticles and SNO nanoparticles

.

3.1 X- Ray Diffraction Analysis:

Figure 1 shows the XRD patterns for undoped NiO, CNO and SNO nanoparticles in the range 2θ = 20°– 80°. The peaks of the undoped NiO sample correspond to the face centered cubic structure (JCPDS file no. 780643). The undoped NiO face centered cubic phase has typical peaks with Miller indices of (100), (200), (220) and (311). The diffractograms of Ce doped NiO nanoparticles and Sm doped NiO nanoparticles also maintained the same face centered cubic structures of NiO and no other crystalline phase was detected. It indicates that the Ce and Sm doping do not change the crystal structure of NiO. The absence of any cerium oxide and samarium oxide associated peaks in the diffractograms signals the successful incorporation of Ce and Sm into NiO crystal as also reported in our previous report [21]. It also underlines the purity of the sample. Debye-Scherrer formula is used to calculate the average size of these nanoparticles. It is about 27 nm for undoped NiO nanoparticles, 35 nm for 1% cerium doped NiO nanoparticles and 33 nm for 1% samarium doped NiO nanoparticles. Lattice parameters calculated from the X-ray diffraction patterns are 4.1759 Å for the undoped sample of nickel oxide nanoparticles, 4.1922 Å for the cerium doped nickel oxide nanoparticles and 4.1770 Å for the 1% samarium doped nickel oxide nanoparticles.

Sample	Particle size (nm)	Lattice Parameters a = b = c (Å)	% Lattice strain
Undoped NiO	27.57	4.1755	0.0232
1.0% CNO	34.64	4.1922	0.0343
1.0% SNO	33.47	4.1770	0.0733

Figure 1: Summary of particle size, lattice parameters and % Lattice strain for Undoped, 1.0 % Ce doped and 1.0 % Sm doped NiO Nanoparticles.

The ionic radii of Ni^{2+}, Ce^{3+} and Sm^{3+} are 69 pm, 114 pm and 108 pm respectively. During the substitutional doping small Ni ions get replaced by bigger Ce and Sm ions which results into the increase in the lattice parameter. In addition, a local distortion is also produced and hence lattice strain is introduced in the lattice. This causes expansion in the lattice. All these results are tabulated in table 1 above.

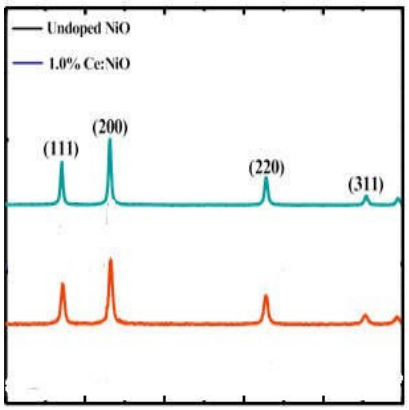

Figure 1: X-Ray Diffraction Pattern for Undoped and 1.0% Ce doped NiO nanoparticles

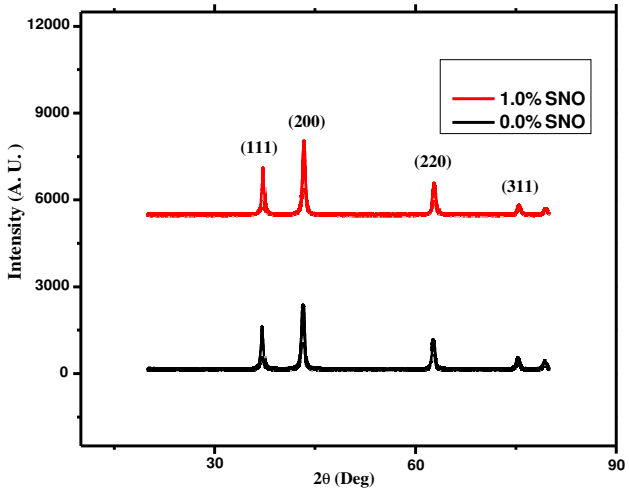

Figure 2: X-Ray Diffraction Pattern for Undoped and 1.0% Sm doped NiO nanoparticles

3.2 EDS Analysis:

The purity of the as-prepared samples is checked by the EDS mapping. The EDS results of CNO and SNO samples are shown in Figure 2 and Figure 3 respectively. These mappings unambiguously confirm the presence of Ni, Ce, Sm and O elements on the entire surface of the material. It also ensures proper doping of Ce and Sm into NiO nanoparticles.

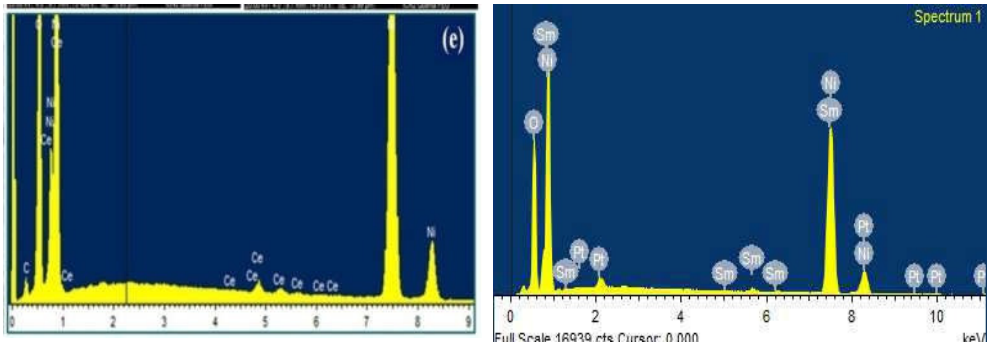

Figure 3: EDS Analysis for 1.0% CNO and SNO nanoparticles

3.3 UV Spectroscopy Analysis:

The optical properties like absorbance and optical band gap energy play an important role in deciding the performance of the nanoparticles in conducting properties. The optical absorption spectra of undoped NiO nanoparticles, 1.0% CNO nanoparticles and 1.0% SNO nanoparticles are recorded at room temperature using UV–visible spectrophotometer available at Physics Department, SPPU. The variation in the absorption density is recorded with change in the wavelength in the range 200-500 nm. The absorption spectra of all the samples are shown in the **Figure 4 and 5**. Extrapolating the linear region of the $(\alpha h\nu)^2$ Vs $h\nu$ curve to the energy axis, the optical band-gap energy of the sample was estimated. The band gap energy for undoped, 1.0% CNO and 1.0% SNO was found as 3.875 eV, 3.502 eV and 3.769 eV respectively.

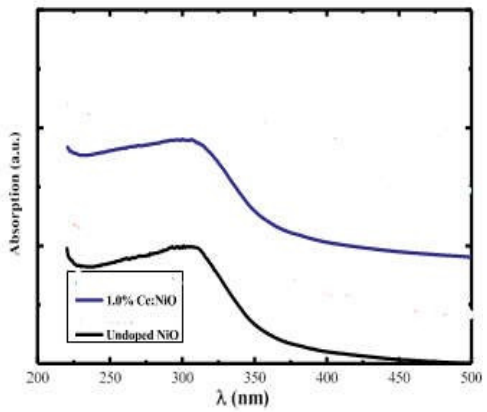

Figure 4: UV Results of Undoped and 1.0% CNO nanoparticles

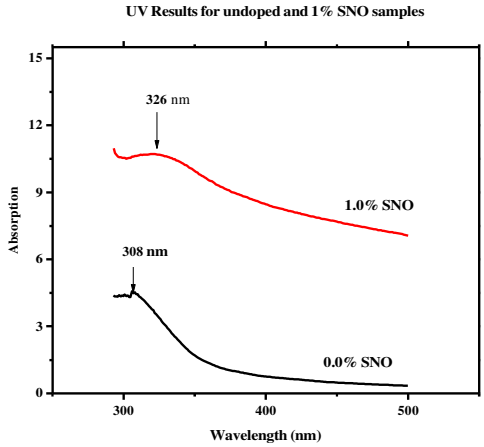

Figure 5: UV Results of Undoped and 1.0% SNO nanoparticles

From the optical properties it is observed that when cerium and samarium are doped into the NiO nanoparticles, the energy band-gap changes. In both the materials it is observed that the band gap decreases with comparison of the undoped NiO material. For cerium doping it decreases from 3.875 eV to 3.502 eV whereas for samarium doping it decreases slightly from 3.875 eV to 3.769 eV. Thus CNO material is more conductive than the SNO material.

4. Conclusions:

Undoped cerium doped and samarium doped nickel oxide nanoparticles are successfully synthesized by sol-gel method. The doping of cerium and samarium is successfully conducted for 1.0% samples. The particle size is found to increase from 28 nm to 35 nm and from 28 nm to 33 nm for 1.0% CNO and 1.0% SNO nanoparticles respectively. The decrease in the bang gap energy along with the doping is observed for both the samples there by making the material more conductive and suitable for semiconducting applications.

5 References:

[1] F. J. Morin. Physical review, 93 [6] (1954) 1199-1204.
[2] W.J. Duan, S. H. Lu, Z. L.Wu and Y. S. Wang. J. Phys. Chem. C 116 (2012) 26043-26051.
[3] L. Yuan, Z. P. Guo, K. Konstantinov, P. Munroe and H. K.Liu. Electrochemical and Solid State Letters. 9(11) (2006) 524-528.
[4] A. C. Patil, A. I. Inamdar, P. S. Shinde, H. P. Deshmukh, R. S. Patil and P. S.Patil. J. Alloys Compd. 489 (2010) 667-673.
[5] C.G. Granqvist, G.A. Niklasson, and A. Azens. Electrochromics. Applied Physics A-Materials Science & Processing. 89 (1) (2007) 29-35.
[6] H. Ohta, M. Hirano, K. Nakahara, H. Maruta, T. Tanabe, M. Kamiya, T. Kamiya and H. Hosono. Appl. Phys. Lett. 83 (2003) 1029-1031.
[7] J. G. Cheng and G. Meng. Rare Metals. 26 (2) (2007) 110-117.
[8] C. Y. Lee and R.-H. Ma. Sensors and Actuators B-Chemical. 122(2) (2007) 503-510.
[9] J. Bandara and H. Weerasinghe. Solar Energy Materials and Solar Cells. 85 (3) (2005) 385-390.
[10] S. S. Shendage, V. L. Patil, S. P. Patil, S. A. Vanalakar, J. L. Bhosale, J. H.Kim and P. S. Patil. J. Anal. Appl. Pyrolysis. 125 (2017) 9-16.

[11] D. K. Bandgar, S. T. Navale, S. A. Vanalkar, J. H. Kim, N. S. Harale, P. S. Patil and V. B. Patil. Synth. Met. 195 (2014) 350-358.
[12] H. Xuemei, S. Yukun and Bai Bo. J. Nanomater. 2016.
[13] C. Feng, X. Kou, X. Liao, Y. Sun and G. Lu. RSC Adv. 7 (2017) 41105 – 41110.
[14] L. F. Koao, H. C. Swart and F. B. Dejene. J. Rare Earths 28 (2010) 206–210.
[15] X. Liu, Y. Zuo, L. Li, X. Huang and G. Li. RSC Adv. 4 (2014) 6397–6406.
[16] M. Yousefi, M. Amiri, R. Azimirad and A.Z. Moshfegh. J. Electroanal. Chem. 661 (2014) 106-112.
[17] P. Anjali, R. Wani, T. S. Sonia, A. Nair Sreekumaran, S. Ramakrishna, R. Ranjusha, K.R.V. Subramanian, N. Sivakumar, C. Gopi Mohan, V. Nair Shantikumar and A. Balakrishana. Sci. Adv. Mater. 6 (2014) 1–8.
[18] Y. J. Li, K.M. Wang, C.I. Kuo and L.J. Chen. Sensors Actuators B 161 (1) (2012) 734–739.
[19] L. Liao, H. X. Mai, Q. Yuan, H. B. Lu, J. C. Li, C. Liu, C. H. Yan, Z. X. Shen and T. Yu. J. Phys. Chem. C 112 (2008) 9061−9065.
[20] A. Ganesan, R. Ganesan, M. Thaiyan, N. Mani, A. Mukkannan and H. Yasuhiro: J. Phys. Chem. C 118 (40) (2014) 23335–23348.
[21] Swati R. Gawali, V. L. Patil, V. G. Deonikar, S. S. Patil, D. R. Patil, P. S. Patil and Jayashree Pant. 'Ce doped NiO nanoparticles as selective NO_2 gas sensor.' Journal of Physics and Chemistry of Solids 114 (2018) 28–35.
[22] J. Yu, K. Chen, X. Chen, H. Wang and D. Xue. Mater. Focus 4 (2015) 81-83.
[23] Huang L, Jha A, Shen S. Spectroscopic properties of Sm^{3+} doped oxide and fluoride glasses for efficient visible lasers (560–660 nm). Opt. Commun. 281 (2008) 4370- 4373.
[24] Kurita A, Kushida T, Izumitani T, Matsukawa M. Persistent spectral hole burning is observed in Sm^{2+} doped glasses at room temperature. Opt. Lett. 19 (1994) 314.
[25] Thamri, S., Sta, I., Jlassi, M., Hajji, M. & Ezzaouia, H. Fabrication of ZnO–NiO nanocomposite thin films and experimental study of the effect of the NiO, ZnO concentration on its physical properties. Mat. Sci. Semicond. Process 71, 310–320 (2017).
[26] Seid, E. T. & Dejene, F. B. Co-solvent medium volume ratio effect on the properties of refluxed sol-gel synthesized ZnO nanopowder. J. Alloys Compd. 787, 658–665 (2019).